Aggregate Structure and Effect of Phthalic Anhydride-Modified Soy Protein on the Mechanical Properties of Styrene-Butadiene Copolymer

Lei Jong

Department of Agriculture, National Center for Agricultural Utilization Research, 1815 N. University St., Peoria, Illinois 61604

Received 10 March 2010; accepted 25 May 2010
DOI 10.1002/app.32870
Published online 25 August 2010 in Wiley Online Library (wileyonlinelibrary.com).

ABSTRACT: The aggregate structure of phthalic anhydride (PA) modified soy protein isolate (SPI) was investigated by estimating its fractal dimension from the equilibrated dynamic strain sweep experiments. The estimated fractal dimensions of the filler aggregates were less than 2, indicating that these particle aggregates have a distorted or broken two-dimensional sheet-like structure. The results also indicated that the aggregate structure has a greater effect on the composite reinforcement than the overall aggregate size. Tensile strength, elongation, Young's modulus, and toughness of hydrolyzed/modified soy composites are comparable with those of carbon black reinforced composites at 10–15% filler fraction. The moduli of PA-modified SPI composites were less sensitive to the pH of the composite preparation compared to the unmodified SPI. The composites prepared at acidic pH, with lower filler fraction, or filled with hydrolyzed/modified SPI are more elastic and less fatigue. The composites of PA-modified SPI had better recovery properties when prepared at acidic instead of alkali pH. PA-modified hydrolyzed SPI composites prepared at acidic pH showed a similar recovery property to that of carbon black reinforced composites, but with greater shear elastic moduli.
 J Appl Polym Sci 119: 1992–2001, 2011

Key words: composites; reinforcement; rubber; mechanical properties; soy

INTRODUCTION

Stability and sustainability of global economy require the use of renewable resources. Agricultural materials are one of the renewable resources that can contribute to the sustainability of material applications. For practical applications (seals, tires, dampers, etc.), carbon black derived from the nonrenewable sources of petroleum or natural gas is the dominating filler used to reinforce crosslinked rubber materials. Some biomaterials have been investigated as fillers in rubber composites, such as starch/rubber composites[1–4] and cellulose/rubber composites.[5–8] We have investigated dry soy protein and carbohydrates that are rigid and have potential to be used as rubber reinforcements. Preliminary studies on different soy products blending with rubber latex to form composites showed substantial reinforcement effects as measured by rheological and mechanical methods. Although the use of these unmodified soy products directly is most cost effective, these polymer blends of unmodified soy products tended to show a more rigid structure due to strong filler networks.[9,10] It was concluded that modification of soy products may be necessary to adjust the blend properties. The change of surface properties of fillers will change filler-matrix interface and therefore composite properties. In this study, soy protein modified by phthalic anhydride that introduced aromatic structure onto soy protein surface and attached to the protein surface through the reaction with amine functional groups is used as a rigid component in a soft polymer matrix to investigate the blend properties. Phthalic anhydride-modified soy protein isolate[11,12] is a readily available commercial product mainly used in paper coating applications. The objective of this study is to examine the effect of such modification of the protein on the composite properties and to obtain structure information. Although green chemistry is desirable for all material components, it is not the objective of this study to address all components with green synthetic routes. However, in this case, known synthetic routes showed that phthalic anhydride could also be derived from renewable sources by the oxidation of *o*-xylene catalytically converted from octadienols, which in turn can be made from 1,3-butadiene converted from bio-ethanol using metal oxides. In practical applications, conventional rubber formulations

Correspondence to: L. Jong (lei.jong@ars.usda.gov).
Names are necessary to factually report on available data; however, the USDA neither guarantees nor warrants the standard of the product, and the use of the name by USDA implies no approval of the product to the exclusion of others that may also be suitable.

may include different types of rubber latices, crosslinking agents, coupling agents, and plasticizers. Because many components are used in a product formulation, it is scientifically difficult to understand the role of a particular component in a more quantitative manner because complex interactions occurred simultaneously. For simplicity, a carboxylated styrene-butadiene (SB) latex containing a small amount of carboxylic acid monomer units was used as the polymer matrix, which crosslinked through the aggregation of ionic functional groups without the complication of covalent reactions such as random crosslinking with sulfur or peroxides. Another objective of using the simple system is to be able to derive aggregate structure of soy protein from dynamic mechanical properties as well as to understand filler-filler and filler-polymer interactions. Although many requirements are needed in a specific application, the reinforcement effect is the major property that needs to be investigated for a new bio-filler as soft polymer reinforcement. With a more clear understanding of reinforcement mechanism, an efficient use of bio-fillers will be possible. Although the system used in this study is model-like, it yields information on the fraction of carbon black filler that can potentially be substituted with modified soy protein filler. In this study, the major physical properties investigated were stress-strain behaviors, dynamic modulus, and dynamic recovery behavior.

EXPERIMENTAL

Materials

Phthalic anhydride-modified soy protein isolates (SPI) were manufactured by reacting phthalic anhydride with aqueous SPI dispersion under alkaline condition.[11,12] Two modified SPI, Pro-Cote 4200 (PC4200) and Pro-Cote 5000 (PC5000) obtained from Solae, LLC, St. Louis, MO were used in this study. PC4200 was an unhydrolyzed and phthalic anhydride-modified SPI and PC5000 was a hydrolyzed and phthalic anhydride-modified SPI. Sodium hydroxide, used to adjust pH, was ACS grade. The carboxylated styrene-butadiene (SB) latex was a random copolymer of styrene, butadiene, and a small amount of carboxylic acid containing monomers (Rovene 9410, Mallard Creek Polymers, Charlotte, NC). According to the manufacturer specification, the glass transition temperature and the styrene/butadiene ratio of the latex are -56°C and 25/75, respectively. The dried latex was not known to be soluble in any solvent or combination of solvents. The latex as received had $\sim$ 50.5% solids and a pH $\sim$ 8.6. The volume weighted mean particle size of the latex was $\sim$ 150 nm.

Preparation of composites

PC4200 or PC5000 was dispersed in water and cooked at 55°C for 1 h. The mean aggregate size and distribution of these dispersions were measured by using a Horiba LA-930 laser scattering particle size analyzer with a red light wavelength of 632.8 nm and a blue light wavelength of 405 nm. The instrument has a measurement range of 0.02–2000 μm. At pH 9, the swollen PC4200 aggregates in aqueous dispersion had a number and volume average size of $\sim$ 15 and $\sim$ 8 μm, respectively; and the swollen PC5000 aggregates had a number and volume average size of $\sim$ 17 and $\sim$ 9 μm, respectively. The volume-weighted particle size of SB latex was $\sim$ 0.15 μm. The dispersions of PA-modified SPI were mixed homogeneously with carboxylated styrene-butadiene latex at 10%, 20, 30, and 40% filler concentration and at pH 9 or 5.2 to form composites. The homogeneous composite mixtures were then quickly frozen in a rotating shell freezer at about -40°C, followed by freeze-drying in a freeze-dryer. The freeze-dried crumb was then compression molded in a window-type mold at 138 MPa and 140°C for 2.5 h. After compression molding, the samples were relaxed and annealed at 90°C and 140°C for 24 h at each temperature. Because water is a plasticizer for soy protein and has an effect on their moduli, the additional drying ensures the samples were compared in dry state without the effect of moisture. To compare the rubber properties of composites reinforced by the modified soy protein with those of carbon black, an aqueous dispersion of carbon black *N*-339 (Sid Richardson Carbon Co., Fort Worth, TX) was prepared by dispersing $\sim$ 100 g of carbon black (CB) in water with the aid of a surfactant, sodium lignosulfonate (Vanisperse CB, Lignotech USA, Rothschild, WI). The weight fraction of the surfactant based on carbon black is 3%. The dispersion was homogenized at 1.2×10^4 rpm for 1 h. The resulting CB dispersion had a solid content of 11.5%. The number and volume average size of CB aggregates were measured to be 280 and 540 nm, respectively.

Stress–strain measurements

Dry samples were stamped ASTM D638 Type V test specimens with a dumbbell shape. Stress–strain measurements were conducted on an Instron 4201 tensile testing machine at a crosshead speed of 1 mm/min and a 1 KN load cell. One to three specimens were measured for each sample. Tensile strength, elongation, Young's modulus, and toughness were obtained from the stress–strain curves. Toughness is defined as energy to break point divided by the specimen volume.

Dynamic mechanical measurements

Both linear and nonlinear viscoelastic properties in shear mode were studied with a control-strain

rheometer. A Rheometric ARES-LSM rheometer (TA Instruments, Piscataway, NJ) with TA Orchestrator software v 7.1.2.3 was used for the dynamic mechanical measurements. All data presented in this study were based on the measurements of one well-prepared sample. To study thermal mechanical properties of the composites, temperature ramp experiments were conducted with torsion rectangular geometry at a heating rate of 1°C/min in the temperature range of −70 to 140°C. When torsion rectangular geometry was used, torsional bars with dimensions of $\sim 50 \times 12.5 \times 6$ mm^3 were mounted between a pair of torsion rectangular fixtures, and the dynamic mechanical measurements were conducted at a frequency of 0.16 Hz (1 rad/s) and a strain of 0.05%. The low frequency and strain used in these measurements caused the modulus response of these samples to occur in the linear viscoelastic region, which was verified by independent strain sweep tests. One well-prepared specimen was used for each composite measurement. The uncertainty of the modulus measurements mainly arose from the uncertainty in the measurement of the specimen dimension. The dimensions of rigid specimens can be more accurately measured in comparison with those of softer specimens. The uncertainty was estimated to be within ±10%.

To study the stress softening effect, strain sweep experiments were conducted using a torsional rectangular geometry to measure the oscillatory storage modulus [$G'(\omega)$] and oscillatory loss modulus [$G''(\omega)$]. The shear-strain-controlled rheometer was capable of measuring the oscillatory strain down to 3×10^{-5} % strain. The rheometer was calibrated in terms of torque, normal force, phase angle, and strain using the instrument's standard procedure. A rectangular sample with dimensions of $\sim 25 \times 12.5 \times 6$ mm^3 was inserted between the top and bottom fixtures. The gap between the fixtures was ~ 7 mm to achieve a strain of ~ 14%. A sample length shorter than 5 mm is not desirable because of the resulting shape change from the clamping at both ends of the sample. The frequency used in the measurements was 1 Hz. The oscillatory storage and loss moduli were measured over a strain range of ~ 0.007–14%, which was incremented by 40 equally spaced data points per decade on a logarithmic scale. The residence time at each strain was automatically controlled by the instrument. The actual strain sweep range was limited by sample geometry and motor compliance at a large strain and by the transducer sensitivity at a small strain. The data that was out of the transducer range was rejected. Although harmonics in the displacement signal may be expected in a nonlinear material, a previous study[13] indicated that the harmonics are not significant if the shearing does not exceed 100%. Each sample was conditioned at 140°C for 30 min to reach an equilibrated dimension and then subjected to eight cycles of dynamic strain sweep to study the stress softening effect. The delay between strain cycles was 100 s. For clarity, only data from the first, fourth, and eighth cycles are presented in the figures. To measure the recovery behaviors at 140°C, the original storage modulus (G_0') of the samples was first measured at 0.05% strain and 0.16 Hz (1 rad/s). Then, the samples were subjected to a large strain of 10% for 30 s and followed by periodic measurements of G' at 0.05% strain and 0.16 Hz (1 rad/s) to record the recovered modulus.

RESULTS AND DISCUSSION

Aggregate structure of phthalic anhydride-modified soy protein

In this study, the aggregate structure of the modified soy protein was estimated by measuring the residual structure of the composites after they were subjected to the cyclic strain experiments. The residual structure is defined as a reversible structure after the composites were subjected to dynamic strain cycles and had reached an equilibrium state. In the current experiments, eight strain cycles were imposed on the samples to obtain equilibrated modulus-strain curves. Because these strain curves are similar in their features, one way to compare these curves is to fit the data to a mathematical model and to compare the fitting parameters. Historically, Payne[14–16] reported the reduction of shear elastic modulus with increasing strain on carbon black filled rubbers in the early 1960s. Later Kraus[17] proposed a phenomenological model based on Payne's postulation of filler networking. The model is based on the aggregation and deaggregation of carbon black agglomerates. In this model, the carbon black contacts are continuously broken and reformed under a periodic sinusoidal strain. On the basis of this kinetic aggregate forming and breaking mechanism at equilibrium, elastic modulus was expressed as follows:

$$\frac{G'(\gamma) - G'_\infty}{G'_0 - G'_\infty} = \frac{1}{1 + (\gamma/\gamma_c)^{2m}} \quad (1)$$

where γ is the applied strain, G'_∞ is equal to $G'(\gamma)$ at very large strain, G'_0 is equal to $G'(\gamma)$ at very small strain, γ_c is a characteristic strain where $G'_0 - G'_\infty$ is reduced to half of its zero-strain value, and m is a fitting parameter related to filler aggregate structures. Equation (1) has been shown to describe the behavior of $G'(\gamma)$ in carbon black filled rubber reasonably well.[18] The loss modulus and loss tangent, however, did not have good agreement with experiments,[19] likely because of the uncertainty in the formulation of a loss mechanism.

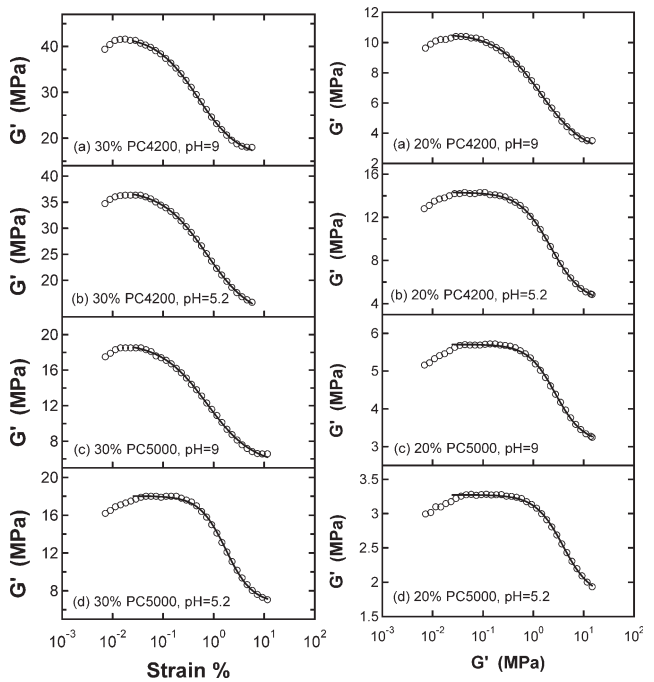

Figure 1 The composites with 30% filler. The eighth cycle of strain sweep experiments at 140°C and 1 Hz are shown. For clarity, the number of data points, represented by circles, is reduced, and the solid lines are fitted from the Kraus model.

The physical meaning of m in the Kraus model may be obtained from the recent studies by Huber et al.,[19] who modeled the Payne effect based on the cluster-cluster aggregation (CCA) model. They obtained $m = 1/(C - d_f + 2)$, where C is a connectivity exponent related to the minimum path along the cluster structure and d_f is the fractal dimension of clusters. Therefore, the fitting parameter m has a physical meaning related to filler network structures that include immobilized polymer chains. The fitting of reversible strain sweep data to the Kraus model is shown in Figure 1.

The model fit and standard deviation of the fit coefficients in Table I were based on 99.73% confidence level with Igor Pro 6.0 software. This model fitting analysis was performed to analyze the residual structures only after the initial structure has been broken down by the dynamic cycles. In general, a smaller fitting parameter m indicates a continuous decrease in G' with increasing strain and suggests a smoother and continuous breakup of filler network structure as the strain is increased. On the other hand, a larger m indicates a more elastic structure at lower strains, which does not yield until a certain strain is applied. When m values are similar between two composites, it was observed that a smaller γ_c value was related to a composite that is less elastic and breaks down substantially at smaller strains.[9,10] The characteristic strain γ_c therefore has a physical meaning associated with the brittleness of the composite structures. From Figure 1 and Table I, the fitting using the Kraus model was generally acceptable, except when a significant G' maximum occurred in the small strain region, which gave rise to a greater uncertainty in m values (Table I). Theoretically, the model did not take into account the G'' transition in the very small strain region ($< \sim 0.02\%$ strain), which can be clearly seen in Figure 2(a,b). Therefore, we chose to start the fitting range from 0.025% strain without taking into account the initial curvature of the strain curves shown in Figure 1.

The m values of 30% filled composites in Table I are in the range of 0.5–0.8. Within different 30% filled composites, PC5000 (5.2) had the largest m value, indicating its filler-related network structure is more resilient than the other composites. General trend also shows that m values of 20% filled composites are greater than those of 30% filled composites as expected because 20% filled composites have a more elastic filler-related network structure. γ_c of the composites showed a general trend that 20% composites are more elastic than 30% composites and PC5000 composites are more elastic than PC4200 composites.

TABLE I
Fitting Parameters of Shear Elastic Modulus[a]

Composition	Best fit[b] m	γ_c (%)	G_0' (MPa)	G_∞' (MPa)	$\Delta G'/G_0'$ [c]
30% filler					
PC4200 (9.0)	0.53 ± 0.02	0.48 ± 0.02	42.3 ± 0.30	15.6 ± 0.40	63%
PC4200 (5.2)	0.49 ± 0.01	0.73 ± 0.02	37.4 ± 0.16	12.7 ± 0.34	66%
PC5000 (9.0)	0.48 ± 0.02	0.74 ± 0.03	19.1 ± 0.16	5.29 ± 0.22	72%
PC5000 (5.2)	0.82 ± 0.03	1.73 ± 0.05	18.1 ± 0.06	6.68 ± 0.19	63%
20% filler					
PC4200 (9.0)	0.50 ± 0.02	1.41 ± 0.05	10.6 ± 0.05	2.61 ± 0.12	75%
PC4200 (5.2)	0.70 ± 0.02	2.22 ± 0.04	14.3 ± 0.03	4.15 ± 0.10	71%
PC5000 (9.0)	0.80 ± 0.04	2.73 ± 0.11	5.71 ± 0.02	3.10 ± 0.06	46%
PC5000 (5.2)	0.79 ± 0.04	3.86 ± 0.21	3.27 ± 0.01	1.79 ± 0.05	45%

[a] The data are from the eighth strain cycle measured at 140°C.
[b] Best fit of shear elastic modulus versus strain with the Kraus Model.
[c] Modulus reduction, $\Delta G'/G_0' = (G_0' - G_\infty')/G_0'$.

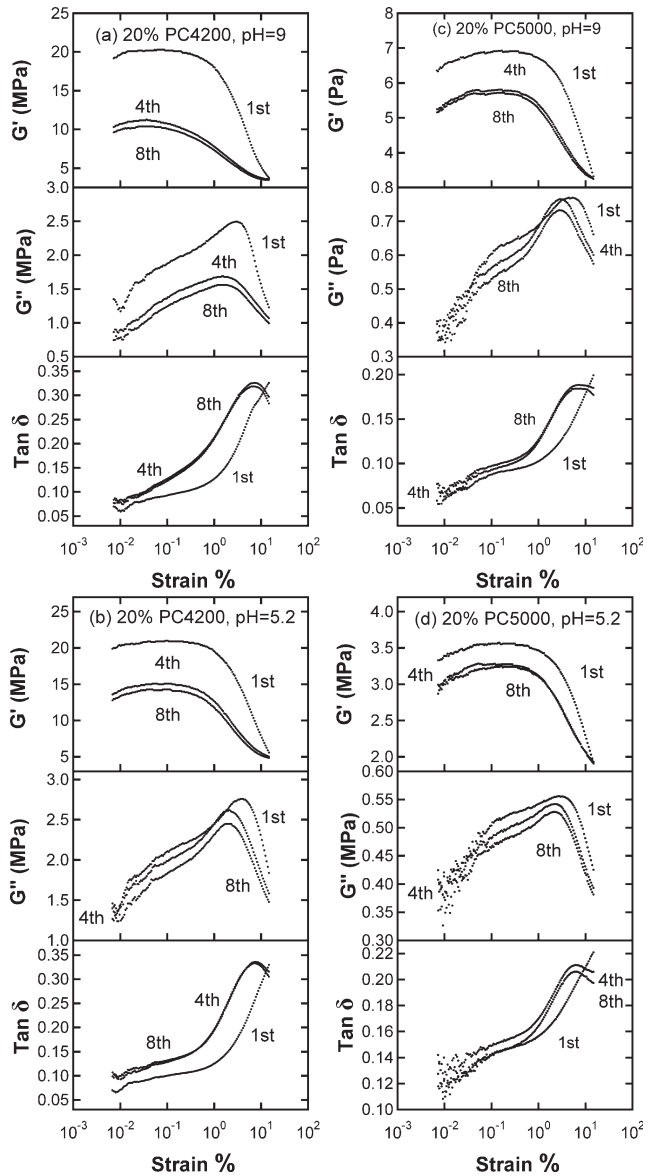

Figure 2 Strain sweep experiments of composites reinforced with 20 wt % filler at 140°C. For clarity, only first, fourth, and eighth strain cycles are shown.

$\Delta G'/G'_0$ values in Table I are the indicator of how much G' was reduced relative to their small strain G' by the imposition of larger dynamic strains. The values show that the moduli of the composites prepared at alkaline pH tended to have greater strain dependence in the larger strain region than the composites prepared at acidic pH. The explanation of this observation is that the composites prepared at alkaline pH are reinforced mainly through a filler network structure that includes more direct bonding between fillers, while the composites prepared at acidic pH are reinforced by a filler network structure that includes more filler-matrix interactions.

Another question needs to be answered is the large aggregate sizes of both PC5000 and PC4200, which appears to give reinforcement effect beyond their sizes are capable of. To understand this, one will need to know the aggregate structure of PC5000 and PC4200. The aggregate structure can be estimated by the combination of dynamic mechanical experiments and the fractal theory associated with these experiments.[18] The fractal dimension of clusters, d_f, can be estimated by using the relationship mentioned above, $m = 1/(C - d_f + 2)$. The results are shown in Table II. The structure of filler aggregates can also be analyzed by estimating the fractal dimensions from the slopes in Figure 3(a), but with volume fraction instead of weight fraction. The weight fractions were converted to volume fractions by the use of component densities, where the density of SB, PC4200, and PC5000 are 1.00, 1.37, and 1.32 g/cm^3, respectively. The fractal dimensions were then obtained using the relationship $(3 + C)/(3-d_f) = \text{slope}$[20,21] and compared with those obtained from m values. A good agreement was obtained between fractal dimensions estimated from the 20% filled composites measured by the strain sweep experiments and those from the slopes of linear viscoelastic measurements. The fractal dimensions obtained from these composites are approximately less than or equal to 2, which indicates that these particle aggregates have a distorted or broken two-dimensional sheet-like structure instead of a compact three-dimensional sphere. This type of structure gave rise to a much larger surface area for filler-filler and filler-matrix interactions compared to that of a compact three-dimensional sphere. This explanation is in agreement with the known knowledge that highly structured carbon black aggregates generate a larger reinforcement effect than compact aggregates. In the experimental side, disagreement was observed for the 30% PC4200 (5.2) and PC5000 (9) composites. The reason for these discrepancies is most likely because these samples were so rigid and brittle that their filler aggregate structure fractured during the strain sweep experiments when the applied strains were too large. These discrepancies indicate that the samples must be elastic enough or the applied strain must be small enough so that the filler aggregates do not fracture during the strain sweep experiments to obtain reliable values of fractal dimensions. In Table II, PA-modified SPI is also compared to unmodified SPI from our previous studies. The comparison indicates that the PA-modification did not change the fractal dimension of SPI significantly despite it increased the aggregate size of SPI. Because the reinforcement effect of PA-modified SPI is similar to that of unmodified SPI (Fig. 3), it can be concluded that reinforcement effect is more closely related to the filler aggregate structure than the overall size of aggregates.

Stress–strain behaviors

The large strain behaviors of these composites were investigated by tensile measurements. Four

TABLE II
Estimated Fractal Dimensions of the Filler Aggregates[a]

	d_f (30% filler)[b]	d_f (20% filler)[b]	d_f [Fig. 3(a)][c]
PC4200 (9.0)	1.4 ± 0.1	1.3 ± 0.1	1.4 (R^2 = 0.985)
PC4200 (5.2)	1.3 ± 0.1	1.9 ± 0.1	1.7 (R^2 = 0.975)
PC5000 (9.0)	1.2 ± 0.1	2.0 ± 0.1	1.8 (R^2 = 0.995)
PC5000 (5.2)	2.1 ± 0.1	2.0 ± 0.1	1.8 (R^2 = 0.986)
	(30% filler)[d]	(20% filler)[d]	Slope[d]
SPI, pH = 9	1.4 ± 0.1	1.5 ± 0.1	1.4 (R^2 = 0.969)
SPI, pH = 5.2	1.7 ± 0.1	1.9 ± 0.2	1.8 (R^2 = 0.993)
HSPI, pH = 9	2.2 ± 0.2	2.3 ± 0.3	1.9 (R^2 = 0.995)
HSPI, pH = 5.2	2.1 ± 0.3	2.1 ± 0.1	–

[a] The measurement temperature is 140°C and $C = 1.3$ is assumed for the connectivity exponent.
[b] Estimated from the 20% and 30% filled composites in Figure 1 using the equation $m = 1/(C - d_f + 2)$.
[c] Estimated from the slopes in Figure 3(a) using the equation $(3 + C)/(3 - d_f)$ = slope, but with volume instead of weight fraction. R^2 is the coefficient of determination, indicating how closely the estimated slopes for the linear lines correspond to the data.
[d] From Ref. 22, where HSPI was referred to hydrolyzed SPI.

properties including tensile strength, elongation, Young's modulus, and toughness were measured and summarized in Figure 4. The results show that the composite tensile strength increases with the increasing filler content in the composites, where PC5000 (5.2) showed a similar behavior to that of CB composites. The composites reinforced with hydrolyzed soy protein isolate (HSPI (9)) prepared in a previous study[22] is also included in the comparison. HSPI (9) composites showed a greater tensile strength than CB composites. The trends showed that the elongation of the composites decreased as the filler contents were increased. The CB composites had a greater elongation compared to other composites except at 10% filler fraction, where PC5000 (9) and HSPI (9) composites had a greater elongation. The Young's moduli of soy reinforced composites were greater than that of the CB composites and increased sharply with the increasing filler fraction, mainly can be explained by the formation of rigid filler networks through ionic and hydrogen bonds. The toughness expressed as the tensile energy to break per unit volume showed that CB composites were tougher than soy reinforced composites except at 10% filler concentration, where PC4200 (5.2), PC5000 (9), and HSPI (9) showed a higher value of toughness. Overall comparison shown in Figure 4 indicates that PC5000 (5.2) and HSPI (9) at 10–15% filler concentration had comparable mechanical properties compared with those of the CB composites. Because carbon black filler concentration in most rubber applications is below 40%, the current measurements may indicate a potential for hydrolyzed soy fillers to replace up to about 40% of carbon black in most rubber composite applications.

Shear storage modulus

Small strain properties of the composites under this study were investigated by dynamic mechanical measurements. In our dynamic experiments, material strength was defined by the dynamic modulus (yield strength). Temperature dependent modulus is a useful property to determine if the composites can be used in a range of application temperatures. Figure 5 shows that PC4200 and PC5000 composites at four filler concentrations (10, 20, 30, and 40%) had similar temperature-dependent features as that of SB polymer. As temperature increased, their moduli showed an initial drop due to the glass transition of SB polymer, followed by a secondary transition and a rubbery region. The primary glass transition temperature of the SB matrix is at about −50°C. The secondary transition at ~ 0°C was assigned to the ionic aggregation in the SB matrix by the comparison of

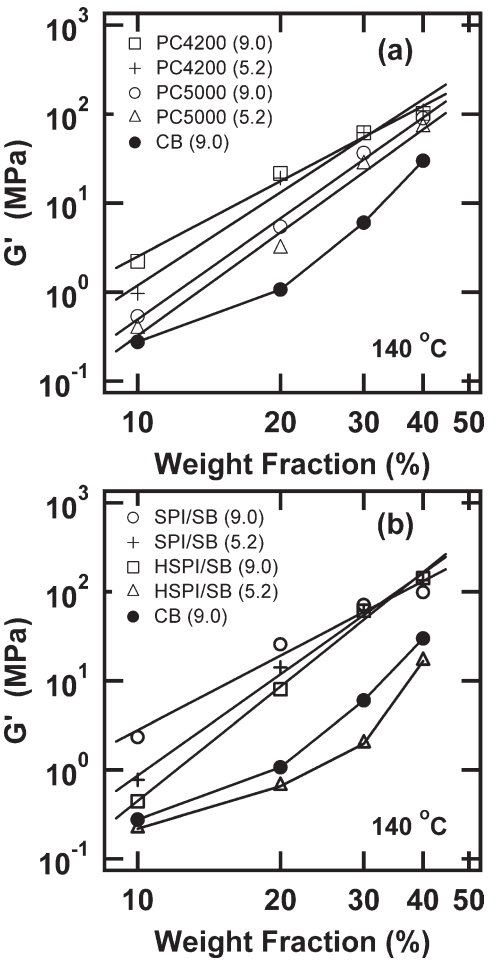

Figure 3 Elastic moduli of (a) modified and (b) unmodified soy composites with different filler concentrations at 140°C.

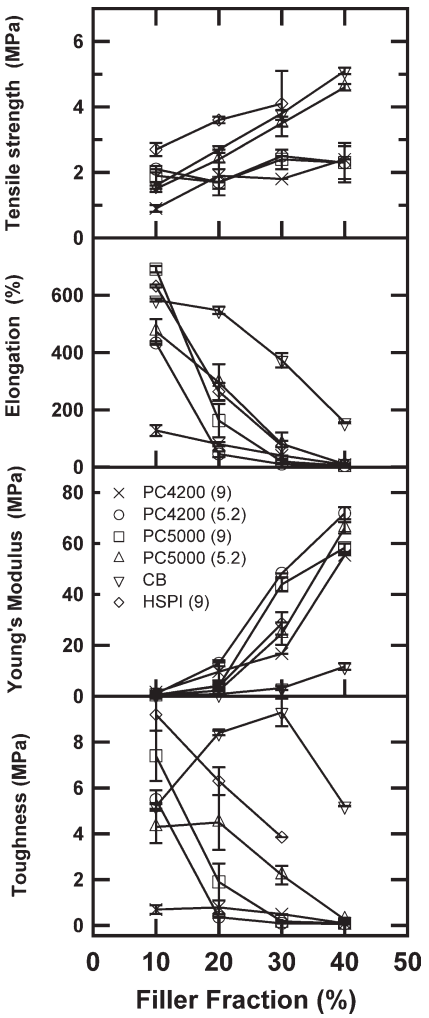

Figure 4 Mechanical properties from stress-strain measurements. The symbols are the same for all figures as those denoted in the figure of Young's modulus.

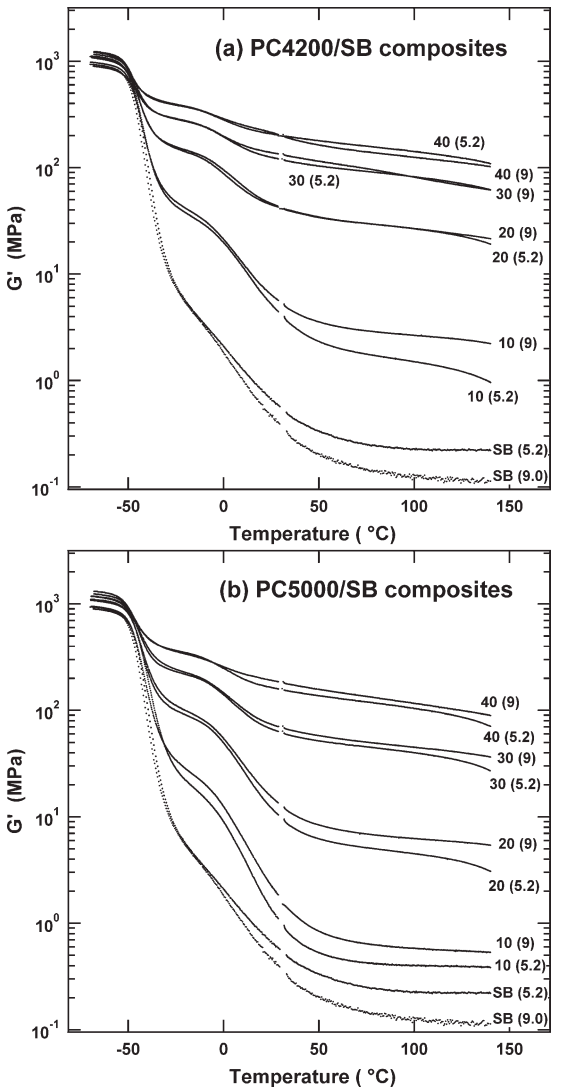

Figure 5 Storage moduli of PC4200/SB and PC5000/SB composites. The weight fraction of filler is shown adjacent to each curve.

styrene-butadiene and carboxylated styrene-butadiene polymers. The moduli of these composites in the rubbery region at 140°C are summarized in Figure 3. The moduli of CB composites from our previous study[22] are also included for comparison. Generally, PC4200 composites have higher modulus values except at higher filler concentrations where they become similar to PC5000 composites at both pH 9 and 5.2. Table III shows that the reinforcement effect of both PC4200 and PC5000 composites prepared at both alkaline and acidic pH is quite significant. Although the SPI composite moduli are higher than that of CB composites, it may not have adequate elasticity for rubber applications. To test the elasticity of the composites, the strain recovery experiments to be discussed later were conducted to determine how well the composites could recover itself from a shear deformation. Compared to CB composites, both PC4200 and PC5000 composites show higher modulus values consistent with their Young's modulus (Fig. 4), likely due to stronger filler related network structure. Figure 3 also shows that the effect of pH on the composite moduli is small by comparing the modulus values of PC4200 or PC5000 at pH 9 and 5.2. This indicates the moduli of PA-modified SPI composites are not as sensitive to the pH of the

TABLE III
The Increase of Composite Modulus Compared with SB at 140°C

Filler fraction	10%	20%	30%	40%
PC4200 (9.0)	20	190	544	905
PC4200 (5.2)	4	87	281	496
PC5000 (9.0)	5	48	322	792
PC5000 (5.2)	2	14	123	322
CB	2	9	53	265

The increase in the modulus is defined as G′(composite)/G′(SB) at the same pH for both composite and SB. The moduli of SB are different at pH = 9 and 5.2.

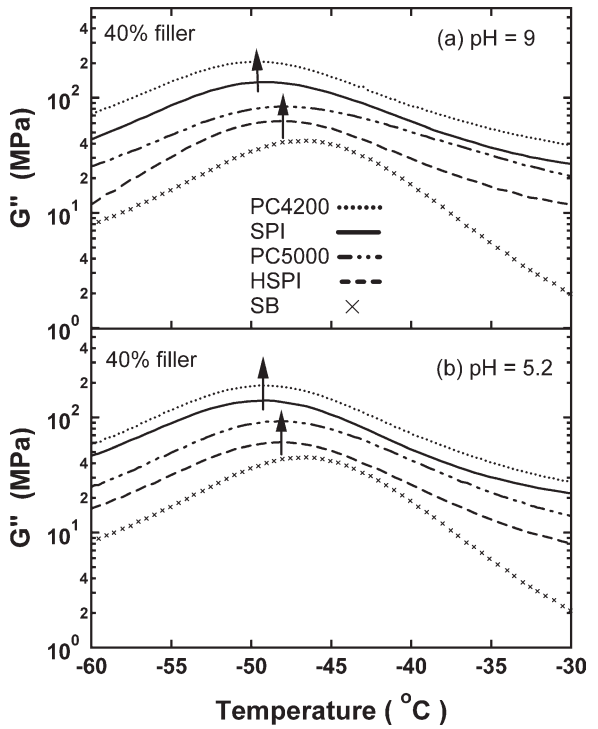

Figure 6 The glass transition temperatures indicated by the loss moduli of the composites with 40% filler and SB matrix. For clarity, the curves were vertically shifted.

preparation as those of unmodified SPI composites. A better understanding can be gained by comparing Figures 3(a,b), which shows our previous study on the unmodified, both hydrolyzed and unhydrolyzed, SPI composites.[22] In that study, it showed that the pH used in the preparation of the composites had a significant effect on the composite modulus, especially for highly hydrolyzed SPI reinforced composites. Comparing the effect of modification and hydrolysis, the latter appears to have a more significant effect on changing the composite moduli. The effect of hydrolysis also produced protein aggregates that have greater ability to immobilize polymer chains and cause the glass transition temperature to shift to a higher temperature as shown in Figure 6. Although the extent of T_g shifting is small, almost the same T_g was obtained for both modified and unmodified SPI composites with 40% filler. The fact that PA modification did not cause the T_g shifting may be an indication that the filler-matrix interactions were not affected by the PA modification.

Fatigue and recovery behaviors

The fatigue properties of these composites provide an understanding on the resilience of the composites and were investigated by stressing the composites with consecutive dynamic strain cycles. The effects are shown in the representative Figure 2 for the composites filled with 20% filler. About 30% filled composites showed a similar trend. The 10% filled and 40% filled composites were not measured because they were either too soft or too rigid to produce reliable data from the strain sweep experiments. To understand these apparently similar strain curves, two characteristics will be discussed: (1) the effect of strain cycle on G' retention (2) the shifting of G'' maximum (G'' max) along the strain axis.

The retention of G' in the small strain region after the eight cycles of strain deformation was used to characterize the fast recovery behavior during the experiment. These data, shown graphically in Figure 2, are summarized in Table II, which shows that 20% composites retain more of the original modulus than 30% composites for PC5000 composites, likely due to a more flexible filler network structure through the incorporation of more polymers. It also shows that the composites prepared at acidic pH tended to have higher modulus retention than those prepared at alkaline pH. Since Figure 6 already showed that the filler-matrix interactions are not affected by PA modification, it is likely that the better moduli retention is caused by a more flexible filler network, which was formed with a more elastic filler-filler interaction.

Twenty percent filled composites had more rubber regions incorporated into the filler network structure, and thus had a more flexible structure and better rebound. In the case of PC4200, the structure is more brittle and tended to cracked if the applied strain were to exceed a certain value. In the strain cycle experiments, the maximum applied strain was 15% for the 20% PC4200 composite and was 6% for the 30% PC4200 composite (Table IV) to avoid visible fractures after the applied strain cycles. This explains why 30% PC4200 composite had slightly better modulus retention than 20% PC4200 composite. However, it was not known if invisible fractures occurred in these samples.

For loss modulus under consecutive strain cycles, the energy dissipation processes of the composites (Fig. 2) became less pronounced and their maxima were shifted from a larger strain to a smaller strain. The structure responsible for the energy dissipation

TABLE IV
The Retention of G' After Eight Strain Cycles[a]

Filler fraction	20%	30%
PC4200 (9.0)	51% (15%)	72% (6%)
PC4200 (5.2)	68% (15%)	73% (6%)
PC5000 (9.0)	83% (15%)	37% (12%)
PC5000 (5.2)	93% (15%)	81% (12%)

[a] The values are the ratio of G' of the eighth strain cycle to that of the first strain cycle at 0.05% strain. Maximum applied strain used for each composite in the strain cycle experiments is indicated in the parentheses.

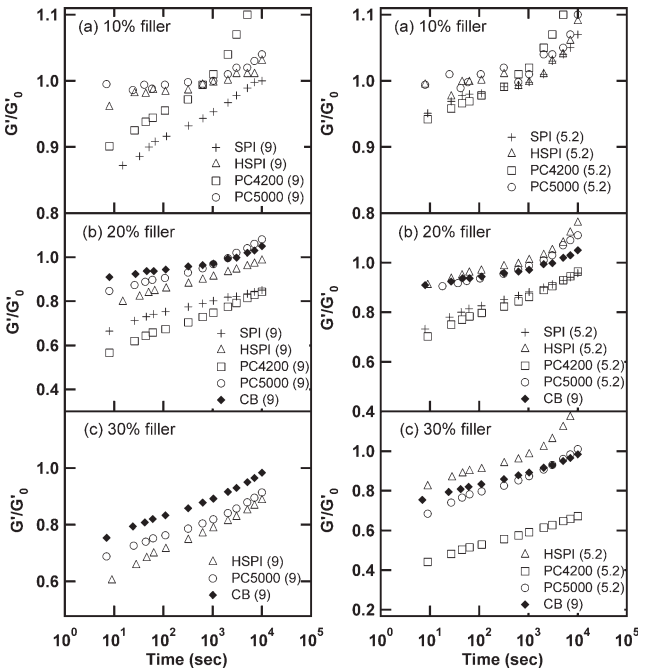

Figure 7 Modulus recovery of the composites with 10–30% filler measured at 140°C.

process is obviously reduced after the eight strain cycles. A loss maximum of a composite that occurs at a larger % strain indicates a more resilient structure, which requires a greater extent of deformation to break down the filler-related network structure. The "filler-related network structure" is defined here as a network formed through the connectivity of fillers and immobilized polymer chains. In such description, the effect of interfaces from filler-filler and filler-polymer interactions is already incorporated and contributes to the modulus of filler-related network structure. The data shows that 20% composites have a G"max occurred at a larger strain than 30% composites, indicating their filler-related network structure was more elastic.

Loss tangent, tan $\delta = G''/G'$, is a measure of the ratio of energy lost to energy stored in a cyclic deformation. The 30% composites are not compared here because different strains were applied on PC4200 and PC5000 composites (Table IV). For 20% composites (Fig. 4), the values of the strain-dependent tan δ from PC5000 composites were lower than those of PC4200 composites. The decrease of the tan δ may be because the decrease of G'' was greater than that of G' as the protein aggregate size was decreased and caused the filler structure to become more elastic. The size reduction through hydrolysis appears to have effect on reducing energy lost in such deformation, possibly because it created more surface area to immobilize polymer chains (Fig. 6). The immobilization of polymer chains in rubbery region often increases the amount of solid-like than liquid-like behavior, which decreases tan δ. However, tan δ being a ratio does not provide information on the composite elasticity or brittleness because it does not directly compare G' or G'' of the composites filled with different size of filler aggregates.

To examine the recovery behavior on these composites, the composites were subjected to a deformation stimulus and allowed to recover from it. Elasticity was defined in our recovery experiments as the extent to which the materials recovered their original modulus. The result is shown in Figure 7. PC5000 composites showed a recovery behavior that was comparable to CB composites in the 20% filled composites and close to CB composites in the 30% filled composites. Both 10 and 20% PC5000 as well as CB composites showed a recovered modulus that is greater than the original modulus ($G'/G'_o > 1$), indicating a structure rearrangement resulting from the application of 10% strain. The description of brittleness and elasticity of the composites is defined in this study as the easiness of the connectivity of the filler network structure to break upon the imposition of a deformation. Better recovery behavior was observed at lower filler concentrations, suggesting that more polymer chains incorporated into the filler-related network structure tended to give better recovery behavior. Comparing the composites prepared at pH 5.2 to those prepared at pH 9, the composites prepared at the acidic pH were more elastic and had better recovery behaviors. In both 20 and 30% filled composites, PC5000 (5.2) composites have a recovery behavior similar to those of CB composites.

CONCLUSIONS

Fractal dimensions of filler aggregates estimated from equilibrated strain sweep experiments indicate that the aggregate structure has a greater effect on the composite reinforcement than the overall size of the aggregates. At 10–15% filled composites, stress-strain measurements indicated that hydrolyzed PA-modified and unmodified SPI had comparable mechanical properties to that of carbon black reinforced composites. The measurement of temperature-dependent shear elastic moduli indicates that the reinforcement effect of PA-modified SPI in the composites is significant and the composite moduli are less sensitive to pH of the composites, compared with our previous studies on the unmodified SPI. However, the magnitude of shear elastic moduli of modified SPI composites over the temperature range studied is similar to that of unmodified SPI composites. Cyclic strain sweep measurements on the composite fatigue indicated that the composites prepared at acidic pH have better modulus retention, the 20% filled composites have a more elastic filler related

network structure than the 30% filled composites, and the composites reinforced by the hydrolyzed/modified SPI have lower energy loss under shear compared to un-hydrolyzed/modified SPI reinforced composites. Strain recovery properties indicated that the composites of PA-modified SPI have better recovery behaviors when they were prepared at pH 5.2 instead of 9. Among these composites, PA-modified hydrolyzed SPI composites prepared at pH 5.2 showed a similar recovery property to that of carbon black composites.

The author thanks Mr. Gary Grose for conducting Instron measurements on these composites.

References

1. Qi, Q.; Wu, Y.; Tian, M.; Liang, G.; Zhang, L.; Ma, J. Polymer 2006, 47, 3896.
2. Wu, Y.; Qi, Q.; Liang, G.; Zhang, L. Carbohydr Polym 2006, 65, 109.
3. Angellier, H.; Molina-Boisseau, S.; Lebrun, L.; Dufresne, A. Macromolecules 2005, 38, 3783.
4. Angellier, H.; Molina-Boisseau, S.; Dufresne, A. Macromolecules 2005, 38, 9161.
5. Yano, S.; Hirose, S.; Hatakeyama, H.; Westerlind, B.; Rigdahl, M. J Appl Polym Sci 1990, 40, 657.
6. Westerlind, B.; Hirose, S.; Yano, S.; Hatakeyama, H.; Rigdahl, M. Int J Polym Mater 1987, 11, 333.
7. Bai, W.; Li, K. Compos A 2009, 40, 1597.
8. Kumar, R. P.; Nair, K. C. M.; Thomas, S.; Schit, S. C.; Ramamurthy, K. Compos Sci Tech 2000, 60, 1737.
9. Jong, L. J Appl Polym Sci 2005, 98, 353.
10. Jong, L. Polym Int 2005, 54, 1572.
11. Meyer, E. W.; Circle, S. J. 1958 U.S. Patent 2,862,918.
12. Krinski, T. L.; Hou, K. C. 2001 U.S. Patent 6,291,559.
13. Chazeau, L.; Brown, J. D.; Yanyo, L C.; Sternstein, S. S. Polym Compos 2000, 21, 202.
14. Payne, A. R. J Appl Polym Sci 1962, 6, 57.
15. Payne, A. R. J Appl Polym Sci 1962, 6, 368.
16. Payne, A. R. J Appl Polym Sci 1963, 7, 873.
17. Kraus, G. J Appl Polym Sci, Appl Polym Symp 1984, 39, 75.
18. Heinrich, G.; Kluppel, M. Adv Polym Sci 2002, 160, 1.
19. Ulmer, J D. Rubber Chem Technol 1995, 69, 15.
20. Huber, G.; Vilgis, T. A. Kautsch Gummi Kunstst 1999, 52, 102.
21. Shih, W.; Shih, W. Y.; Kim, S.; Liu, J.; Aksay, I. A. Phys Rev A 1990, 42, 4772.
22. Jong, L, Peterson, S. C. Compos A 2008, 39, 1768.